Comparative Circular Dichroism Studies of an Anti-Fluorescein Monoclonal Antibody (Mab 4-4-20) and Its Derivatives†

Sergey Yu. Tetin,‡ William W. Mantulin,§ Lisa K. Denzin,‡ Karla M. Weidner,‡ and Edward W. Voss, Jr.*,‡

Department of Microbiology, University of Illinois at Urbana-Champaign, 407 South Goodwin Avenue, and Laboratory for Fluorescence Dynamics, Department of Physics, University of Illinois at Urbana-Champaign, 1110 West Green Street, Urbana, Illinois 61801

Received May 19, 1992; Revised Manuscript Received August 6, 1992

ABSTRACT: This study presents circular dichroism (CD) spectra of a high-affinity monoclonal anti-fluorescein antibody (Mab 4-4-20), its Fab fragments, and corresponding single-chain antibody (SCA). In the region 200–250 nm, the differences in the CD spectra between these proteins reflect the uneven distribution of chromophores (tryptophan and tyrosine) rather than a major conformational change. On the basis of near-UV CD spectra, binding of the hapten fluorescein to these protein antibodies elicits an increased asymmetry in the microenvironment of the chromophoric residues in contact with the hapten and also perturbs the interface between V_L and V_H domains. The hapten-binding site provides a chiral microenvironment for fluorescein that elicits a pronounced induced fluorescein CD spectrum in both the visible and UV regions. In contrast to the parent molecules, SCA is thermolabile. Our results demonstrate that (1) UV CD spectra are useful for assessing the chromophoric microenvironment in the binding portion of antibodies and (2) the extrinsic fluorescein hapten CD spectra provide information about the interaction of hapten with the binding pocket.

The system of fluorescein–anti-fluorescein antibodies has been developed as a model for studies of immunochemical and spectroscopic principles [as reviewed by Voss (1990)]. This system has been relatively well characterized. Bedzyk et al. (1989) reported the primary structure of antibodies belonging to the 4-4-20 idiotype family. Herron et al. (1989) described the three-dimensional structure of the liganded Fab fragments derived from Mab 4-4-20. At the ligand level, the fluorescence properties of the system have been described (Voss, 1984) with emphasis on the specific quenching of hapten fluorescence. Swindlehurst and Voss (1991) found stereospecificity of the antigen-binding site with measurable differences in isomeric hapten binding. Investigation of structural dynamics using time-resolved fluorescence spectroscopy of idiotypically related liganded anti-fluorescein antibodies has been initiated (Bedzyk et al., 1991).

Furthermore, the advent of single-chain antibody (SCA) technology (Bird et al., 1988; Huston et al., 1988; Colcher et al., 1990) has permitted site-specific mutagenesis studies of the 4-4-20 combining site. These studies defined the relative roles of the fluorescein–amino acid contact residues in the variable domains (Denzin et al., 1991), as assessed by hapten fluorescence quenching and spectral shifts in the absorption spectra.

It is clear that further studies are needed to better understand immunoglobulin conformation and especially the in vitro folded SCA in which the synthetic polylinker simulates the structural role of constant domains. SCA is also important for acquiring immunochemical data about induced immunogenic epitopes on liganded anti-fluorescein antibodies, called "metatopes" (Voss et al., 1988). Metatope studies suggest significant conformational changes in the variable domains after ligand binding (Wiedner et al., 1992). Consequently, the fluorescein–anti-fluorescein system also requires supplemental characterization at the protein structural level. The high content of aromatic chromophores, namely, tryptophan and tyrosine residues, and their unique distribution throughout the antibody molecule prompted us to utilize the information contained in the protein's circular dichroism (CD) spectra. CD spectra have often been used as empirical markers of perturbations in immunoglobulin conformation (Rinfret et al., 1985; Buchner et al., 1991).

The phenomenon of induced optical activity of fluorescein after binding to antibodies is of additional interest. This observation was previously described for polyclonal anti-fluorescein antibodies (Gollogly & Cathou, 1974; Voss & Watt, 1977) and can be used to derive important information about contact residues, particularly in the hapten-binding site of a monoclonal antibody population. Therefore, realizing the importance of aromatic chromophores to the immunoglobulin CD spectrum, we report relative circular dichroic effects in the ultraviolet and visible regions of anti-fluorescein high-affinity murine monoclonal antibodies (Mab 4-4-20), papain-derived Fab fragments, and the SCA derivative of Mab 4-4-20.

MATERIALS AND METHODS

Proteins. Monoclonal antibody 4-4-20 (IgG2a,κ; $K_a = 2.5 \times 10^{10}$ M^{-1}) was obtained by affinity purification using fluorescein–Sepharose 4B from mouse ascites fluid as previously described (Kranz & Voss, 1981; Reinitz & Voss, 1984). Fab fragments were prepared by papain cleavage of IgG 4-4-20 and purified on a protein A–Sepharose 4B column as described by Weidner and Voss (1991). The Fab fragments exhibited a binding affinity of 2.3×10^{10} M^{-1} (Weidner, unpublished results). The single-chain antibody (SCA) 4-4-20 [$K_a = (4–5) \times 10^9$ M^{-1}] consisting of the variable heavy- and light-chain domains, tethered by the 14 amino acid residue linker (212 polylinker), was constructed, expressed, and folded

† This work was partially supported by a grant from the Biotechnology Research Development Corp., Peoria, IL. The LFD is supported by the National Center for Research Resources of the National Institutes of Health (RR03155) and by UIUC.

* To whom correspondence should be addressed.

‡ Department of Microbiology.

§ Laboratory for Fluorescence Dynamics, Department of Physics.

0006-2960/92/0431-12029$03.00/0

Table I: Distribution of Tryptophan and Tyrosine in Mab 4-4-20[a]

Ig protein	tyrosine	tryptophan
IgG(κ)2a 4-4-20 total	54	26
Fc	10	8
Fab	22	9
V_H	11	4
V_L	4	2
SCA	15	6
Variable Region–Interdomain Surface (Partially or Fully Exposed Residues)		
V_H	8	3
residue no.	56, 61, 62, 97, 101, 102, 103, 107	33, 47, 108
V_L	3	1
residue no.	37, 41, 54	101

[a] In this paper, we use the sequential numbering system of Herron et al. (1989) and not the commonly encountered scheme of Kabat et al. (1987).

as previously described by Bird et al. (1988) and Denzin et al. (1991). Protein purity was confirmed by SDS–polyacrylamide gel electrophoresis with appropriate markers (Laemmli, 1970). Previously, Bedzyk et al. (1990) immunochemically characterized IgG 4-4-20 and SCA 4-4-20/212 by competitive ELISA and found that each of the antibodies in the nonliganded form showed the same reactivity with an antiidiotypic reagent. After hapten binding, the 4-4-20 proteins reacted equally well with an antimetatypic reagent.

Circular Dichroism (CD) Studies. CD spectra were recorded on the SPEX/Jobin-Yvon Model CD-6 instrument, which was calibrated with a solution of (+)-10-camphorsulfonic acid (CSA). The stock CSA solution showed an optical rotation of $[\alpha]^{20}_D = +21.5°$. The following cuvettes (Hellma) were used in various wavelength regions: 200–250 nm, 0.01- and 0.1-cm path length; near-UV and visible regions, 1.0-cm path length. Each spectrum was averaged 3–5 times and smoothed with Dichrograph Software version 1.1 (Jobin-Yvon Instruments S.A., Paris, France). A spectral acquisition spacing of 0.2 nm (2-nm bandwidth) was used in the 200–250-nm region, and 0.1-nm spacing (1-nm bandwidth) was used in the near-UV and visible regions. Sample absorbance did not exceed 1.0 in the spectral regions measured.

All measurements were performed at 20 °C, and CD spectra at different temperatures for SCA and Fab were performed with a thermostat-controlled sample chamber.

Other Methods. Protein concentrations were determined from absorption spectra (240–350 nm) corrected for light scattering (Levine & Federici, 1982). The spectra were measured with a dual-beam Perkin-Elmer Lambda 5 spectrophotometer and/or with the dichrograph.

The extinction coefficients ($E^{1mg/mL}_{278}$) 1.46, 1.60, and 2.07 for IgG 4-4-20, Fab, and SCA were calculated from the chromophore content in the primary structure (Bedzyk et al., 1989) (see Table I). Fluorescein disodium salt (Molecular Probes) and its derivative 9-hydroxyphenylfluoron, HPF (kindly provided by Dr. W. Ware, University of Western Ontario), have a molar extinction coefficient of $\epsilon_{490} = 72\,000$ M^{-1} cm^{-1}.

The standard buffer in these studies was 0.1 M potassium phosphate, pH 8.0, and all solutions were filtered through 0.22-μm Millipore low protein binding filters.

RESULTS

CD Spectra of Unliganded Proteins in the 200–250-nm Region. Figure 1 shows the CD spectra of IgG 4-4-20, Fab fragments 4-4-20, and SCA 4-4-20 in the 200–250-nm region.

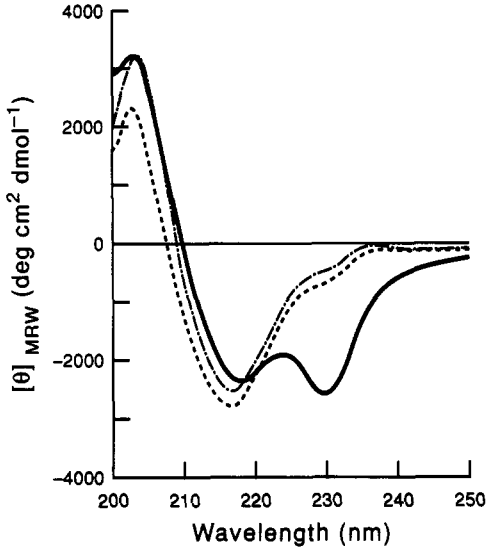

FIGURE 1: CD spectra of unliganded Mab 4-4-20 between 200 and 250 nm: SCA (—), Fab fragments (– · –), and IgG (- - -).

Results are expressed in terms of mean residue weight ellipticity. One positive extremum at 204 nm and two negative extrema at 217 and 230 nm are common to these unliganded proteins. The CD spectra of IgG and isolated Fab fragments display a similar amplitude and shape. It is noteworthy that the negative shoulder at 230 nm in the CD spectra of IgG and Fab fragments is more pronounced in the SCA spectrum and appears as a negative maximum.

Near-UV CD Spectra of Unliganded and Liganded Proteins. Immunoglobulin proteins have a characteristic high content of chromophoric tryptophan (Trp) and tyrosine (Tyr) residues. The primary structure of Mab 4-4-20 determined by Bedzyk et al. (1989) established that there are 9 Trp and 22 Tyr in Fab fragments (Table I). In the two variable domains, which are the basis of SCA, there are 6 Trp and 15 Tyr residues. The heavy-chain isotype of Mab 4-4-20 is IgG2a, and accordingly there are 8 Trp and 10 Tyr in the Fc portion (Kabat et al., 1987). Consequently, for the monovalent molecule of Mab 4-4-20 (1/2 IgG) there are 13 Trp and 27 Tyr residues. If some of these chromophores are located in asymmetric (chiral) microenvironments, then CD spectra in the 250–300-nm region arise.

The near-UV CD spectra corresponding to unliganded IgG, Fab fragments, and SCA are presented in Figure 2. Results are expressed in terms of molar ellipticity (per mole of protein). The IgG and Fab near-UV CD spectra are rather dissimilar in contrast to the CD spectra at 200–250 nm. The positive maximum near 295 nm is common for these proteins. The short-wavelength shoulder (286–289 nm) in the CD spectra of IgG and Fab fragments appears as a small positive maximum at 287 nm in the SCA spectrum.

After hapten binding in the molar ratio 1:1 (1 mol of fluorescein per antigen-binding site), the protein spectra acquire two pronounced positive maxima at 287 and 295 nm (Figure 3). Results are presented per mole of protein for Fab fragments and SCA, but per $^1/_2$ mole of IgG to normalize for the second antigen-binding site. Upon ligand binding the amplitude of the 295-nm peak approximately doubles in each case. Changes in the spectra near 287 nm are large but cannot be quantitated because the peaks are not unequivocally defined in the spectra of the unliganded form (Figure 2). An additional complication to a quantitative interpretation of the liganded protein CD spectra arises from the small contribution of the extrinsic CD of bound fluorescein. This effect also accounts

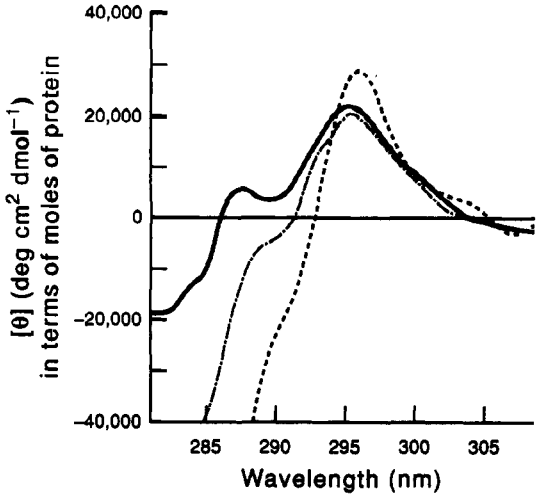

FIGURE 2: CD spectra of unliganded Mab 4-4-20 in the near-UV region: SCA (—), Fab fragments (– · –), and IgG (- - -).

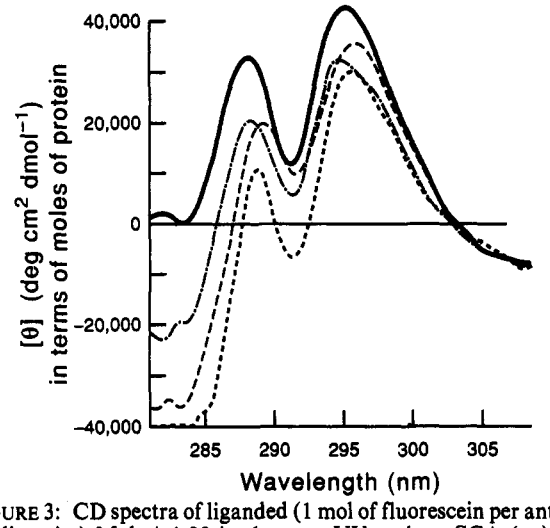

FIGURE 3: CD spectra of liganded (1 mol of fluorescein per antigen-binding site) Mab 4-4-20 in the near-UV region: SCA (—), Fab fragments (– · –), and IgG (- - -). Curve (– –) shows the CD spectra of IgG + HPF in the same ratio. The total ligand concentration in each case is 1.5×10^{-5} M.

for the non-zero CD at 310 nm, a region with no significant protein absorbance.

Since SCA molecules are not structurally stabilized by adjacent constant domains, we anticipate measurable thermal perturbation in their localized chromophoric microenvironments. Earlier studies (Zav'yalov et al., 1977a,b) on V_L dimers from proteolytically cleaved κ-type Bence-Jones protein IVA showed a significant temperature dependence of the chromophore microenvironment. Figure 4 shows the temperature dependence of the amplitude at 295 nm in the CD spectra of unliganded Fab fragments and SCA. The amplitude values from the spectra at each temperature were averaged. The measured effects were reversible. In the temperature range 3–40 °C the $[\theta]_{295}$ for Fab is essentially invariant, but for SCA the curve reaches a plateau at its maximum between 15 and 30 °C. Heating of SCA to 37 °C distorts the CD spectrum and beyond 40 °C induces protein aggregation and precipitation. The dashed line signifies this effect.

CD Spectra of Fluorescein–Antibody Complexes in the Visible Region. An interesting property of fluorescein is its induced optical activity after binding by antibodies. By contrast, there is a lack of optical activity in the absence of binding (Gollogly & Cathou, 1974; Voss & Watt, 1977). Figure 5 compares the CD spectra of fluorescein complexes

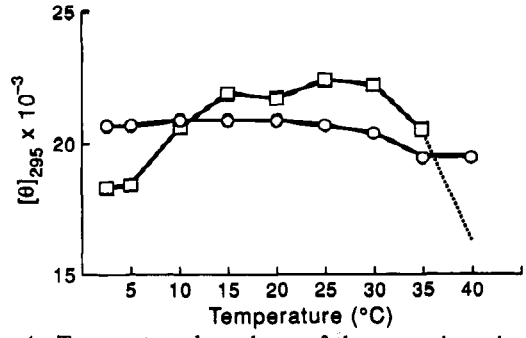

FIGURE 4: Temperature dependence of the spectral maximum at 295 nm in the CD spectra of unliganded Fab fragments (○) and SCA (□). The size of the symbols are commensurate with the magnitude of the standard deviation of the various experiments. $[\theta]_{295}$ is expressed in terms of moles of protein (deg cm² dmol⁻¹). The temperature (°C) scan followed the sequence: 20–3°, 3–38°, 38–20°, 20–38°, 38–3°, and 3–20°.

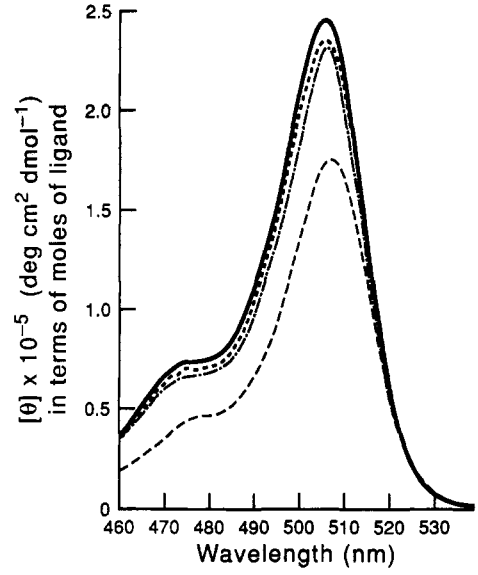

FIGURE 5: CD spectra of fluorescein bound to Mab 4-4-20: SCA (—), Fab fragments (– · –), IgG (- - -), and HPF bounded by IgG (– –). The haptens are added in the ratio of 1 mol of ligand per antigen-binding site. The total ligand concentration in each case is 1.5×10^{-5} M.

with IgG, Fab fragments, and SCA. The results are presented in terms of molar ellipticity of fluorescein for the mole ratio of one hapten per active site. The bound fluorescein CD spectra (maximum at 506 nm) completely correspond to the absorption spectra of the Mab 4-4-20–fluorescein complex in this wavelength region. Even though the binding constant of fluorescein to SCA is approximately 4-fold smaller, relative to IgG (Bedzyk et al., 1990), the amplitude of its CD spectrum at 506 nm is slightly greater. The same effect is observed in the near-UV CD spectra (Figure 3). At equimolar conditions, binding saturation is not achieved. When sufficient protein is added to complex all free ligand (i.e., saturation), the amplitude of the fluorescein-bound SCA CD spectrum ($[\theta]_{506}$ = 258 000 deg cm² dmol⁻¹) exceeds the corresponding amplitude of the IgG spectrum ($[\theta]_{506}$ = 241 000 deg cm² dmol⁻¹).

Towell (1976) postulated that one possible mechanism for fluorescein's induced CD effect involves the electrostatic effect of the phenylcarboxylate moiety. To test this proposition, we measured the CD spectrum of IgG 4-4-20 complexed with a fluorescein analogue, 9-hydroxyphenylfluoron (HPF), which lacks the carboxyl group. The shape and sign of the IgG-bound HPF spectrum are the same as for fluorescein's

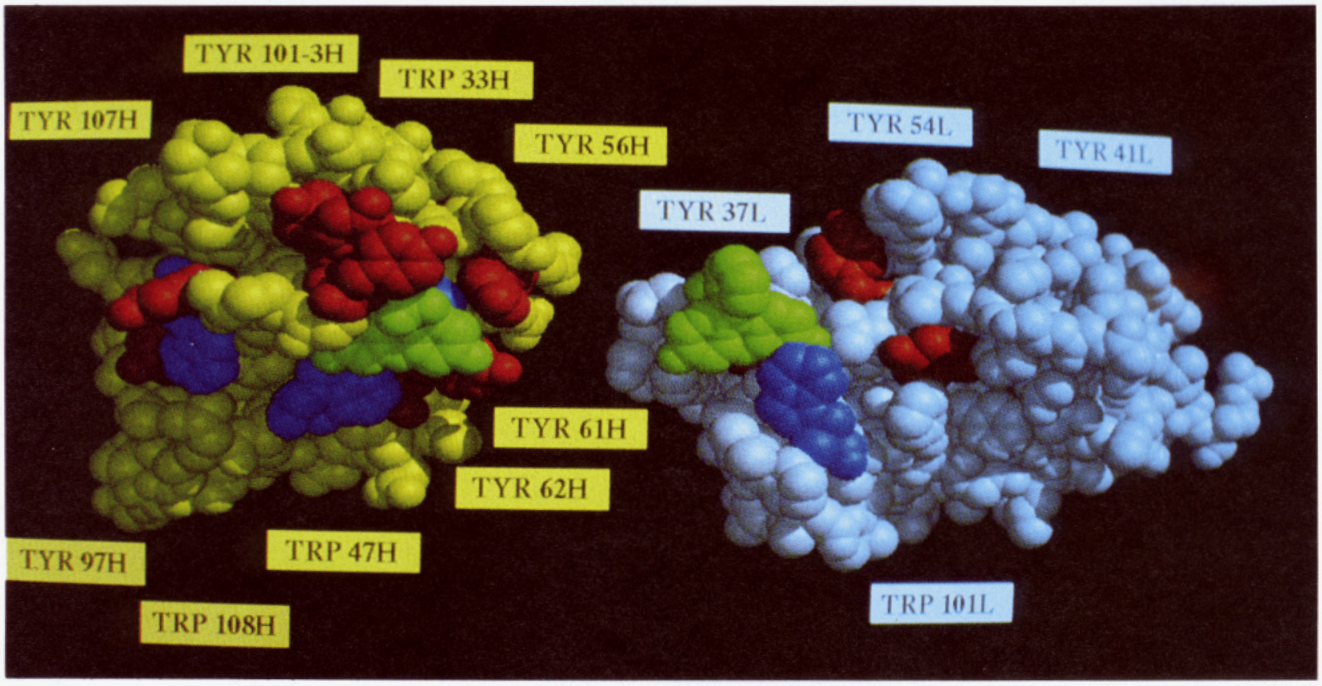

FIGURE 6: Internal surfaces of V_L (white) and V_H (yellow) domains. Tryptophans are blue and tyrosines are red. The hapten (fluorescein) is green. Fluorescein is indicated in both domains, simply to provide a domain orientation; in reality, there is a single hapten bound. This model is constructed from X-ray data of liganded Fab 4-4-20 at 1.7-Å resolution (J. Herron, personal communication).

complexes (Figure 5). The lower amplitude reflects a significantly lower affinity (6.5×10^7 M^{-1}) of HPF for Mab 4-4-20 (Bedzyk et al., 1992).

DISCUSSION

The antibodies we have studied exhibit the characteristic immunoglobulin CD spectrum in the far-ultraviolet region with a peak at 217 nm and a shoulder near 230 nm (Figure 1). Such spectra are typical of proteins with β-structure and a high aromatic content (Woody, 1978; Brahms & Brahms, 1980) and are represented by the superposition of several "primary" CD spectra. The commonly applied algorithms for secondary structure calculations in globular proteins, which do not account for the spectral contribution of aromatic side chains, are consequently inappropriate for immunoglobulin CD spectra. There is both an experimental and a theoretical basis for assigning the gross spectral features in Figure 1 to aromatic chromophore contributions. Delving into the vacuum UV region (163–213 nm), which contains additional spectral bands, Brahms and Brahms (1980) generated CD spectra from a selected basic set of proteins and polypeptides with known β-sheet and β-turn structures determined from X-ray studies. By application of this approach to immunoglobulin proteins, composite spectra provided good agreement with the measured CD spectra for the κ-type Bence-Jones protein dimer (V_{REI}). Spectral agreement was not maintained if the empirically generated spectra included data above 220 nm. They proposed that, in immunoglobulin CD spectra, the negative extremum around 217 nm is typical of β-structure distorted due to a significant contribution of aromatic side-chain chromophores in the CD spectrum above 215 nm.

Theoretical calculations by Woody (1978) support his assignment of CD spectral bands in the 225–230-nm region to the L_a transition of tyrosine residues. Contributions by phenylalanine occur below 220 nm. More recent results (Woody, 1987) indicate that the B_b transition of the tryptophan side chain contributes to the far-UV CD spectra of proteins around 225 nm. In most proteins the sign of both these transitions tends toward the positive, but negative values are predicted in some cases (Woody, 1978, 1987).

Consequently, we suggest that the shoulder at 230 nm in the CD spectra of IgG and Fab fragments and the corresponding negative maximum in the CD spectrum of SCA (Figure 1) are attributable to tyrosine and/or tryptophan side chains. The distinct maximum at 230 nm in the CD spectrum of SCA is evidence for the localization of asymmetric chromophores in the variable domains. The traditional expression of far-UV CD spectra in terms of mean residue ellipticity does not accommodate the uneven distribution of chromophores in the protein. For example, if the amplitude of the 230-nm maximum is calculated in terms of protein molar ellipticity, rather than mean residue ellipticity, the resulting amplitudes for SCA and Fab are identical.

The localized concentration of asymmetric chromophores in the variable domains is supported by the near-UV CD spectra (Figure 2). In this region the maximum at 295 nm is common to the proteins. When the results are calculated in terms of the molar protein concentration, the peak at 295 nm shows the same amplitude for Fab fragments and SCA. The intensity of the 295-nm maximum in the Fab spectrum (Figure 2) is approximately two-thirds of the maximum value in the CD spectrum of IgG, since IgG consists of three fragments, two Fab and one Fc, each with the same molecular weight.

It is difficult to assign amplitude contributions to specific tryptophan or tyrosine residues, but generally the extinction of tryptophan is much larger at 295 nm. In IgG there are approximately three times as many tyrosines as tryptophans, and the bands between 285 and 290 nm, where both chromophores show commensurate absorption, may reflect a significant tyrosine contribution.

Ligation of the antibodies by fluorescein results in similar near-UV CD spectra with well-resolved spectral maxima (Figure 3) and significantly larger amplitudes than for the unliganded proteins (Figure 2). This spectral similarity is supplementary evidence for the localized concentration of

asymmetric chromophores in the variable portion of Mab 4-4-20.

The distribution of tryptophan and tyrosine residues in the variable domains of Mab 4-4-20 deserves particular attention. According to X-ray data for liganded Fab fragments (Herron et al., 1989; J. N. Herron, personal communication), the internal surfaces involved in V-domain interactions are rich in aromatic residues (Table I and Figure 6). In the V_H domain three of four tryptophan residues (Trp 33, 47, 108) and eight of eleven tyrosine residues (Tyr 56, 61, 62, 97, 101, 102, 103, 107) are partially or fully exposed at the interdomain surface. Similarly, in V_L one of two tryptophans, Trp 101, and three of four tyrosines, Tyr 37, 41, and 54, are also on the interfacial surface. The high concentration of aromatic residues on these surfaces, which direct domain–domain interactions, may also provide favorable packing constraints. The unique topography of tryptophan and tyrosine residues may contribute to complex interactions of indole and phenol rings necessary to achieve the correct orientational pairing of variable domains. It is important to note that components of both surfaces form the antigen-binding site and TrpH33 is one of the contact residues involved in hapten binding (Herron et al., 1989). By contrast, there are no tyrosine or tryptophan residues at the domain interface of C_L and C_H1.

One explanation for the increased amplitude in the near-UV CD spectra of liganded antibodies (Figure 3) invokes the increasing asymmetry of aromatic residues (TrpH33, TrpL101, and TyrL37) in contact with the hapten, but the magnitude of the spectral effect accommodates additional mechanisms. Fluorescein by virtue of its high affinity and large size can induce perturbation throughout the variable portion, including the highly aromatic interdomain surfaces. This concept is supported by a significant change in the effective radius of SCA 4-4-20 after hapten binding (Weidner et al., 1992). Furthermore, Herron et al. (1991) report crystallographic studies showing a small displacement of variable domains in BV04-01 autoantibodies upon single-stranded DNA binding. It is noteworthy that the light-chain structure in these autoantibodies differs from Mab 4-4-20 in only six positions and only two substitutions occurred in the CDR (complementarity-determining regions). Voss et al. (1992) proposed a model of epitope origins, both idiotype and metatype, which involves a dynamic mechanism for the variable domain's unliganded and liganded status. In this case, significant conformational perturbation and stabilization during ligand binding were postulated.

Another approach to investigate the Mab 4-4-20 binding site relates to the spectral properties of liganded fluorescein. Free fluorescein possesses no optical activity but acquires it after binding by antibodies. The induced CD spectrum of fluorescein fully tracked the absorption spectrum of the IgG-bound hapten, in terms of both the wavelength of observed spectral peaks and the relative intensities in the 320–540-nm region (data not shown). Between 270 and 310 nm the absorption spectrum of fluorescein is weak and featureless. We suspect that the induced CD of fluorescein in this wavelength region may slightly skew the liganded protein CD spectra of Figure 3. From our measurements, the difference in optical density (ΔA) at 506 nm of bound fluorescein between right- and left-hand circularly polarized light (positive amplitude in the CD spectrum) is approximately 0.1% of the total absorption. Gollogly and Cathou (1974), as well as Voss and Watt (1977), described the induced optical activity of bound fluorescein with polyclonal antibodies. The sign and amplitude of induced fluorescein CD spectra varied for different polyclonal antibody preparations. The structure of fluorescein, which includes the planar xanthenone rings and phenylcarboxylate moiety, is relatively rigid; however, crystallographic data (J. N. Herron, personal communication) indicate a slight distortion of the rings, and thus the observed induced optical activity arises from a mixed origin, both inherent and interactive Cotton effects. By definition, the interactive extrinsic optical activity of a bound ligand is due to interactions with an asymmetric environment in the binding site and results in the observed spectral perturbations (Towell, 1977; Edwards, 1979). Towell (1977) proposed the one-electron mechanism as one of several explanations for the induced optical activity of protein-bound fluorescein and phthalein dyes. This mechanism involves the charge of the phenylcarboxylate moiety and consequently is inconsistent with the extrinsic CD of HPF (Figure 5), which lacks the carboxyl group. Earlier work by Athey and Cathou (1977) on the binding of various 6-hydroxyxanthen-3-ones to polyclonal antibodies is consistent with our conclusion about the generation of induced CD spectra even in the absence of a phenyl or phenylcarboxylate substituent on the hydroxyxanthenone ring structure. It should be noted that our fluorescein-bound Mab 4-4-20-induced CD spectra differ in sign and amplitude in some wavelength regions from the polyclonal antibody studies of Athey and Cathou (1977), since the polyclonal antibodies contain a large pool of variable protein structures. Edwards and Woody (1983), as well as Athey and Cathou (1977), highlighted the role of the tryptophan side chain as the dominant contributor to extrinsic optical activity of bound dye chromophores. In the Mab 4-4-20 system TrpH33 and/or TrpL101 fulfill(s) this role. Furthermore, we cannot dismiss the possible involvement of charged groups HisL31 and especially ArgL39 in the binding pocket on the appearance of an induced CD spectrum.

The properties of SCA require specific discussion. The SCA 4-4-20/212 based on Mab 4-4-20 variable domains, linked by 14 residues through V_L (COOH) and V_H (NH_2) sites, is not stabilized by constant domains. After in vitro folding SCA retains all immunochemical characteristics, like idiotypes and metatypes of the parent protein, and only the 4–5-fold reduction in the hapten binding constant of SCA indicates some structural differences with IgG (Bedzyk et al., 1991). On the basis of CD studies two additional differences are noted. First, the conformational lability of SCA's chromophore environment shows a significant dependence on temperature (Figure 4) and an anomalously low temperature (around 40 °C) of denaturation, resulting in precipitation and aggregation. The second observation relates to hapten accommodation in the SCA binding site. The CD spectral results in the near-UV and visible regions for the antibody–hapten complexes discriminate a relatively enhanced amplitude for SCA, both at equimolar and at saturating (visible region) conditions. Presumably, the labile conformation of SCA results in a more pronounced spectral response to hapten binding. In conclusion, our results show that CD spectroscopy in the UV and visible regions is useful in comparing conformational properties of free and liganded Mab 4-4-20. The extrinsic CD of the fluorescein hapten will be applied to the determination of equilibrium binding constants of anti-fluorescein antibodies and mutagenized SCA proteins.

ACKNOWLEDGMENT

We thank J. N. Herron for providing the 1.7-Å resolution structural model for liganded Fab 4-4-20 and R. W. Woody for his insight and helpful discussions. The CD measurements

were performed at the Laboratory for Fluorescence Dynamics (LFD) at the University of Illinois at Urbana-Champaign (UIUC).

REFERENCES

Athey, T. W., & Cathou, R. E. (1977) *Immunochemistry 14*, 397–404.

Bedzyk, W. D., Johnson, L. S., Riordan, G. S., & Voss, E. W., Jr. (1989) *J. Biol. Chem. 264*, 1565–1569.

Bedzyk, W. D., Weidner, K. M., Denzin, L. K., Johnson, L. S., Hardman, K. D., Pantoliano, M. W., Asel, E. D., & Voss, E. W., Jr., (1990) *J. Biol. Chem. 265*, 18615–18620.

Bedzyk, W. D., Swindlehurst, C. A., & Voss, E. W., Jr. (1992) *Biochim. Biophys. Acta 1119*, 27–34.

Bird, R. E., Hardman, K. D., Jacobson, J. W., Johnson, S., Kaufman, B. M., Lee, S. M., Lee, T., Pope, S. H., Riordan, G. S., & Whitlow, M. (1988) *Science 242*, 423–426.

Brahms, S., & Brahms, J. (1980) *J. Mol. Biol. 138*, 149–178.

Buchner, J., Renner, M., Lilie, H., Hinz, H.-J., & Jaenicke, R. (1991) *Biochemistry 30*, 6922–6929.

Colcher, D., Bird, R. E., Rosseli, M., Hardman, K. D., Johnson, S., Pope, S., Dodd, S. W., Pantoliano, M. W., Milenic, D. E., & Schlom, J. (1990) *J. Natl. Cancer Inst. 82*, 1191–1197.

Denzin, L. K., Whitlow, M., & Voss, E. W., Jr. (1991) *J. Biol. Chem. 266*, 14095–14103.

Edwards, R. A. (1979) Ph.D. Thesis, Colorado State University, Fort Collins, CO.

Edwards, R. A., & Woody, R. W. (1983) *J. Phys. Chem. 87*, 1329–1337.

Gollogly, J. R., & Cathou, R. E. (1974) *J. Immunol. 113*, 1457–1467.

Herron, J. N., He, X., Mason, M. L., Voss, E. W., Jr., & Edmundson, A. B. (1989) *Proteins 5*, 271–280.

Herron, J. N., He, X., Ballard, D. W., Blier, P. R., Pace, P. E., Bothwell, A. L. M., Voss, E. W., Jr., & Edmundson, A. B. (1991) *Proteins 11*, 159–175.

Huston, J. S., Levinson, D., Mudget-Hunter, M., Tai, M., Novotny, J., Margolies, M. N., Ridge, R. Y., Bruccoleri, R. E., Huber, E., Crea, R., & Opperman, H. (1988) *Proc. Natl. Acad. Sci. U.S.A 85*, 5879–5883.

Kabat, E. A., Wu, T. T., Reid-Miller, M., Perry, H. M. & Gottesman, K. S. (1987) *Sequences of Proteins of Immunological Interest*, U.S. Department of Health, Bethesda, MD.

Kranz, D. M., & Voss, E. W., Jr. (1981) *Mol. Immunol. 18*, 889–898.

Laemmli, U. K. (1970) *Nature 227*, 680–685.

Levine, R. L., & Federici, M. M. (1982) *Biochemistry 21*, 2600–2606.

Reinitz, D. M., & Voss, E. W., Jr. (1984) *Mol. Immunol. 21*, 775–784.

Rinfret, A., Horne, C., Dorrington, K. J., & Klein, M. (1985) *J. Immunol. 135*, 2574–2581.

Swindlehust, C. A., & Voss, E. W., Jr. (1991) *Biophys. J. 59*, 619–628.

Towell, J. F., III (1977) Ph.D. Thesis, Colorado State University, Fort Collins, CO.

Voss, E. W., Jr., Ed. (1984) *Fluorescein Hapten: An Immunological Probe*, CRC Press, Boca Raton, FL.

Voss, E. W., Jr. (1984) *Comments Mol. Cell Biophys. 6*, 197–221.

Voss, E. W., Jr., & Watt, R. M. (1977) *Immunochemistry 14*, 237–241.

Voss, E. W., Jr., Miklasz, S. D., Petrossian, A., & Dombrink-Kurtzman, M. A. (1988) *Mol. Immunol. 25*, 751–759.

Voss, E. W., Jr., Weidner, K. M., & Denzin, L. K. (1992) *Immunol. Invest. 21*, (1) 71–83.

Weidner, K. M., & Voss, E. W., Jr. (1991) *J. Biol. Chem. 266*, 2513–2519.

Weidner, K. M., Denzin, L. K., & Voss, E. W., Jr. (1992) *J. Biol. Chem. 267*, 10281–10288.

Woody, R. W. (1978) *Biopolymers 17*, 1451–1467.

Woody, R. W. (1987) in *Proceedings of the Federation of European Chemical Societies Second International Conference on Circular Dichroism* (Kajtar, M., Ed.) Budapest, Hungary, pp 38–56, VCH Publishers, New York.

Zav'alov, V. P., Demchenko, A. P., Suchomudrenko, A. G., & Troitsky, G. V. (1977a) *Biochim. Biophys. Acta 491*, 7–15.

Zav'alov, V. P., Troitsky, G. V., Khechinashvili, N. N., & Privalov, P. L. (1977b) *Biochim. Biophys. Acta 492*, 102–111.

Registry No. Trp, 73-22-3; Tyr, 60-18-4; fluorescein, 2321-07-5.